NANOELECTRONIC CHEMICAL SENSORS FOR CHEMICAL AGENT AND EXPLOSIVES DETECTION

R.R. Smardzewski [1,*], N.L. Jarvis[2] A.W. Snow[3], H.Wohltjen[4]

[1]Geo-Centers, Inc., Gunpowder Branch PO Box 68
Aberdeen Proving Ground, MD 21010-0068
[2]U.S. Army Edgewood Chemical Biological Center
Aberdeen Proving Ground, MD 21010-5424
[3]Naval Research Laboratory, Washington, DC 20375
[4]Microsensor Systems, Inc., Bowling Green, KY 42103

ABSTRACT

A new class of nanometer-scale, low power, solid-state devices is being investigated for the detection of CW agents and other hazardous vapors. These nanoelectronic chemical vapor sensors, or "chemiresistors" are comprised of nanometer-sized gold particles (1.2-2.4nm) encapsulated by monomolecular layers of functionalized alkanethiols (R-SH) deposited as thin films on interdigitated microelectrodes (Fig 1).

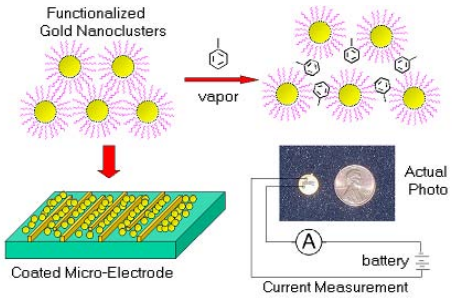

Fig. 1. Nanoelectronic Chemical Sensor Concept.

When chemical (agent, explosive) vapors reversibly absorb into these thin films, a large modulation of the electrical conductivity of the film is observed. The measured current between gold clusters is extremely sensitive to very small amounts of monolayer swelling or dielectric alteration caused by absorption of vapor molecules. For chemical agent simulants, a large dynamic range (5-logs) of sensitivities is observed and extends down to ppb (parts-per-billion) vapor concentrations. For explosive vapors of TNT/DNT detection limits in the femtogram range have been observed. Complete reversibility has been observed for all analyte vapors and the devices exhibit relatively low sensitivity to water vapor (a major interferent). Tailored selectivities of the sensors are accomplished by incorporation of chemical functionalities at the terminal structure of the alkanethiol or substitution of the entire alkane structure.

1. BACKGROUND

Over the past ten years, there has been considerable interest in nanometer-sized materials largely due to the wide range of applications of these materials in several fields including advanced electronics, nonlinear optics, catalysis and hydrogen adsorption[1]. Recent interest in this "intermediate state of matter" stems largely from a seminal 1994 study by Brust et al.[2] where a new method was developed for preparing and stabilizing nanometer-sized gold colloids that are easily dispersed in organic solvents and isolated as pure powders. Colloids have been studied since Faraday's examination of them[3] but they were only stable in solution. Depending on the preparative conditions, the particles had a tendency to agglomerate slowly, eventually lose their disperse character and flocculate. The removal of solvent generally led to the complete loss of the ability to reform a colloidal solution. Brust and coworkers solved this problem by "protecting" the gold colloids or clusters with the self-assembled surfactant, dodecanethiol ($C_{12}H_{25}SH$), which was then well known to form self-assembled monolayers on planar gold surfaces[4]. Leff and coworkers[5] further demonstrated that control of the gold particle size in this system could be achieved by varying the gold-to-thiol reactant ratio and applied a model in which the role of the thiol is analogous to that of the surfactant in water-in-oil microemulsions. In many respects these new cluster compounds behave like simple chemical compounds; they can be precipitated, redissolved and chromatographed[6] without any apparent change in properties. This preparative methodology allowed a reasonable degree of control of the size of the nanoparticles, and most research groups have targeted the technologically-attractive 1-5 nm size range for these monolayer-protected clusters (MPCs).

In 1998, Wohltjen and Snow[7] demonstrated that gold nanoclusters with functionalized protecting monolayers form the basis of sensitive vapor "chemiresistors" by depositing these MPCs to produce metal-insulator-metal-ensemble (MIME) films on interdigitated

Report Documentation Page

Form Approved
OMB No. 0704-0188

1. REPORT DATE	2. REPORT TYPE	3. DATES COVERED
00 DEC 2004	**N/A**	**-**

4. TITLE AND SUBTITLE	5a. CONTRACT NUMBER
Nanoelectronic Chemical Sensors For Chemical Agent And Explosives Detection	5b. GRANT NUMBER
	5c. PROGRAM ELEMENT NUMBER
6. AUTHOR(S)	5d. PROJECT NUMBER
	5e. TASK NUMBER
	5f. WORK UNIT NUMBER
7. PERFORMING ORGANIZATION NAME(S) AND ADDRESS(ES) **Geo-Centers, Inc., Gunpowder Branch PO Box 68 Aberdeen Proving Ground, MD 21010-0068; U.S. Army Edgewood Chemical Biological Center Aberdeen Proving Ground, MD 21010-5424**	8. PERFORMING ORGANIZATION REPORT NUMBER
9. SPONSORING/MONITORING AGENCY NAME(S) AND ADDRESS(ES)	10. SPONSOR/MONITOR'S ACRONYM(S)
	11. SPONSOR/MONITOR'S REPORT NUMBER(S)

12. DISTRIBUTION/AVAILABILITY STATEMENT
Approved for public release, distribution unlimited

13. SUPPLEMENTARY NOTES
See also ADM001736, Proceedings for the Army Science Conference (24th) Held on 29 November - 2 December 2005 in Orlando, Florida. , The original document contains color images.

14. ABSTRACT

15. SUBJECT TERMS

16. SECURITY CLASSIFICATION OF:			17. LIMITATION OF ABSTRACT	18. NUMBER OF PAGES	19a. NAME OF RESPONSIBLE PERSON
a. REPORT	b. ABSTRACT	c. THIS PAGE			
unclassified	**unclassified**	**unclassified**	**UU**	**7**	

microelectrodes (IMEs) and measuring resistance changes as a function of vapor exposure for a number of chemical vapors. Depending upon the vapor, large, rapid and reversible modulations (both positive and negative) of the electrical conductivity of these thin nanocluster films were observed.[8]

Recently, these sensors have been studied at the Edgewood CB Center (ECBC), jointly with the Naval Research Laboratory (A.W. Snow) and Microsensor Systems, Inc. (H. Wohltjen). Parts-per-million (ppmv) and parts-per-billion (ppbv) sensitivity limits have been obtained for a number of vapors including CW simulants and several agents.[9-10] Vapor selectivities were accomplished by choosing appropriate functionalized thiol surfactants.

2. MATERIALS

The majority of functionalized (i.e. "protected") gold nanoclusters were synthesized by a modification of the original methodology of Brust and coworkers[2]. Products were formed by simultaneous Au(III) reduction (from an $AuCl_4^-$ solution) in the presence of functionalized alkanethiols in a two-phase aqueous/organic system. Sodium borohydride ($NaBH_4$) was used as the reducing agent. The relative rates of nanocluster growth and alkanethiol surface complexation are a function of the initial concentrations of Au(III) chloride and alkanethiol reagents.[11] In the cases described in this paper, a 1:1 molar ratio of reagents was employed which produced gold nanoclusters with an average core diameter of 1.7-nm. This translates into approximately 201 gold atoms per nanocluster (Au_{201}) as determined by others[12] from ^{1}H-NMR line-broadening, high-resolution transmission electron microscopy, small-angle X-ray scattering and thermogravimetric analysis.

For certain compositions that were difficult to prepare by direct synthesis, modifications to a "place-exchange" process[13-14] were employed to incorporate specific functionalized thiols into the nanoclusters. To effect an exchange, an n-alkylthiol stabilized nanocluster was added to a relatively concentrated solution of a selected functionalized thiol. With time, the weakly bound alkylthiols desorbed into the solution to be replaced by those thiol molecules in large excess.

The shell thickness on the nanocluster is determined by the size (chain length) of the alkanethiol reagent. For straight chain $C_4 - C_{16}$ alkanethiols, the corresponding shell thickness ranges from 0.4 to 1.0 nanometers(nm).

Deposition of thin nanocluster films was accomplished by airbrushing dilute colloidal solutions in chloroform or methanol onto interdigitated microelectrodes. Microelectrodes were gold electrode arrays fabricated on 7x12.5x1-mm quartz substrates each consisting of 50 finger pairs of 15μm width, 15μm spacing, 4800μm overlap length and 1500Å thickness. Film thickness estimates were calculated from spectroscopic measurements.

3. ELECTRONIC CONDUCTIVITY

The electronic conductivity between the individual gold nanoclusters is extremely sensitive to increases in the distance of separation of the gold clusters as well as to the very small dielectric changes caused by vapor absorption (Fig. 2).

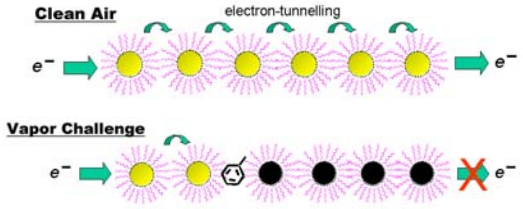

Fig. 2. Intercluster Conductivity Concept.

For the nerve agent simulant DMMP (dimethyl methylphosphonate) a dynamic range of 5-6 logs of sensitivities was observed down to a vapor detection limit of 9-ppbv. To put this limit of detection (LOD) for DMMP in context, 9-ppbv is equivalent to 0.04-mg/m^3 which is comparable to the published[15] M22 ACADA value of 0.1 mg/m^3 for GA and GB at maximum alert response times of < 60-seconds.

Initially, selection of the functionalized surfactants used to optimize nanosensor selectivity and sensitivity for specific vapors and classes of vapors was based primarily on solubility considerations. Preliminary studies using solubility as a guidline resulted in arrays of sensors giving characteristic response patterns for many hazardous vapors at concentrations in the low ppm to ppb range. It was initially believed that vapor absorption in the intercluster medium, and the subsequent swelling of the thin film, would result only in increases in resistance as the distance separating conducting gold nanoclusters was increased. However, it was soon observed that swelling was not the only mechanism by which an absorbed vapor could modulate conductivity in these films. The presence of strong charge-acceptor or charge-donor groups in absorbed vapor molecules could result in large changes in the dielectric (and thus the capacitance) of the intercluster medium as well as modulate the electronic structure of the organic bridge molecules comprising the conducting path between gold clusters. This was clearly demonstrated by the absorption of the strong electron acceptors dinitrotoluene (DNT) and trinitrotoluene (TNT) which produced extraordinary large changes in resistance at extremely low vapor concentrations, and actually increased conductivity of

specific nanocluster films rather than increasing resistance. With the very low vapor concentration of TNT (8.02 x 10^{-6} torr @ 25°C)[16], it was unlikely to have caused significant swelling of the film, which in any case would not account for the large observed *increase* in conductivity. Rapid (> 90% FSD in < 1-3 sec) and reversible changes in both resistance and capacitance were observed for TNT(5% in sand) and DNT(pure solid) headspace vapors exposed to interdigitated electrodes containing three specific films. This is illustrated in Fig. 3 where the DNT response is presented as both capacitance, C and resistance, R vs. time for a 15-20 second vapor challenge at an excitation voltage/frequency of 0.5V/10kHz. The TNT response is given as device impedance (Z') at 0.5V/8kHz versus time for a 20 second vapor challenge. Ambient laboratory air was used in all exposure/purge cycles.

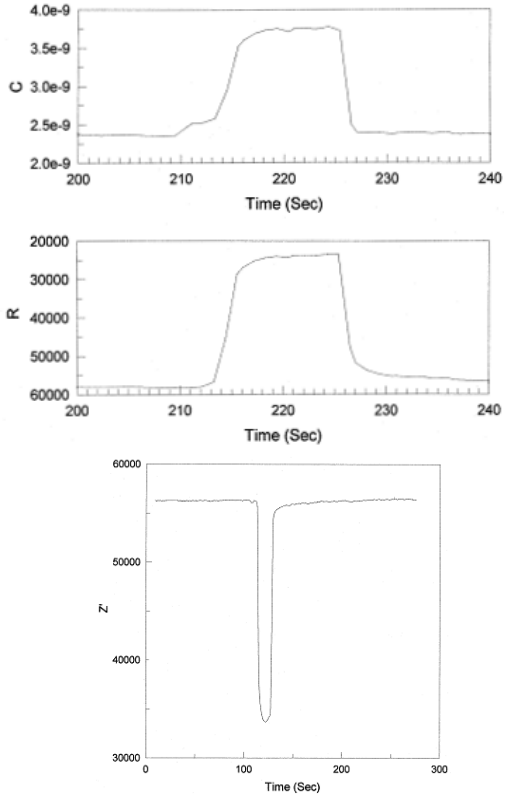

Fig. 3. DNT (upper) and TNT (lower) Headspace Vapor Responses at 25°C.

GC-MS scans, using heated vapor-transfer lines, of these headspace samples taken at temperatures from 33° to 52°C showed only DNT mass peaks increasing with temperature. No lower MW contaminants were observed in the headspace of either DNT or TNT.

The surprising results for TNT and DNT (18X the volatility of TNT)[16] suggested a new approach to the development of thiol-stabilized gold nanoclusters with even greater sensitivity and selectivity for CW agents as well as many other hazardous vapors. It suggested that functionalized surfactants can be designed and synthesized that include strong charge acceptor or donor groups in their structure which selectively interact with charge transfer groups that are present in many hazardous vapors. Complexing of charge transfer groups in both the functionalized surfactant and vapor molecules will greatly alter the dielectric of the interparticle medium, modify the electronic structure of the organic compounds of the conduction path, and produce large changes in the conductivity and capacitance of the films.

4. THEORY

The vapor sensitivity of monolayer stabilized gold nanoclusters results from modulation of electron (or hole) conduction between gold nanoclusters through the interaction of absorbed vapor molecules with the organic media between the nanoclusters. The electronic current through the bridging organic layer is a function of the length of the bridging layer as well as the chemical (electronic) structure of the compounds comprising the conduction path[17]. For example, Han[18], et al. found that arrays of 5-nm Au particles stabilized by 11-mercaptoundecanoic acid had resistances two orders of magnitude greater than 5-nm Au particles stabilized by 1,9-nonanedithiol, even though both structures had approximately the same interparticle spacing. Much as the addition of "doping" molecules can increase the conductivity of highly conjugated organic polymers by several orders of magnitude[19], exposure of the organic bridging molecules to strong charge donor or acceptor vapors can significantly affect the electronic conductivity, as was observed with DNT and TNT vapors. Whereas swelling of a nanocluster film increases cluster/cluster separation and only increases sensor resistance, absorption of strong donor or acceptor molecules can result in either increases or decreases in resistance, as has been observed in our studies.

The electronic conductivity of gold nanocluster films reflects the facility of their electron transport and is similar to that of redox polymers where an electron hopping, or electron self-exchange mechanism is operative. The nanocluster cores are treated as localized donor-acceptor sites on which the electronic charges reside and the thiolate ligand shell, as a dielectric medium surrounding the cores that undergoes repolarization in the course of the electron transfer.

The simplest approach to understanding the conductivity of these nanocluster films is suggested from the classic model of Neugebauer and Webb[20].

$$\underset{Conductivity}{\sigma(T,\delta)} = \underset{\Downarrow}{\sigma_0 \exp(-\delta\beta)}\,\underset{\Downarrow}{\exp(-E/RT)} \qquad (1)$$

$$\qquad\qquad\qquad\qquad\qquad\qquad\qquad\quad \underset{tunneling}{} \qquad \underset{hopping}{}$$

The electronic conductivity (σ) is a function of the temperature (*T*), interparticle nanocluster edge-edge distance (δ), the electron transfer coupling coefficient (β, typically equal to $1Å^{-1}$) and the activation energy (*E*) for the electron hop. There are two contributions to the overall conductivity. The first, exp(-δβ), is a tunneling term associated with electron tunneling between two metallic cores separated by a dielectric, and the second, exp(**-***E/RT***)**, is an activation energy term which is required for the generation of a positively and a negatively charged core from two initially neutral ones, i.e.

$$2MPC^0 \xrightarrow{E} MPC^+ + MPC^- \qquad (2)$$

$$MPC = \text{Monolayer Protected Clusters}$$

The granular metal conductivity model[21-25] has been studied extensively for systems such as 2-2000Å metal (Au, Ag, Ni) grains dispersed below the percolation threshold in a dielectric medium, such as SiO_2 particles of the same size. The theory can be categorized into so-called low-field and high-field conductivity regimes. The nanoclusters examined here fall into the smaller dimension range and our present voltage studies (<1volt) into the low-field regime. Charge carrier generation occurs by the preceding disproportionality equation. In this low-field regime, the activation energy is given by:

$$E = \frac{1}{2}\frac{e^2}{4\pi\varepsilon\varepsilon_0}\left\{\frac{1}{r} + \frac{1}{r+\delta}\right\} \qquad (3)$$

where ε = the dielectric constant of the intervening medium, ε_0 = vacuum dielectric constant, ***e*** = electron charge, r = radius of nanocluster core and δ = interparticle nanocluster edge-edge distance.

From a consideration of the preceding equations, It is readily apparent that any process that alters the core-core separation (δ) or the dielectric constant (ε) of the intervening medium between the cores will be readily detectable by following changes in the conductivity. Furthermore, as the dielectric constant of the medium is increased, with all other parameters remaining constant, the activation energy (*E*) will be decreased and hence conductivity (σ) increased. This is exactly what happens for the highly polar vapor analytes of DMMP, TNT and DNT, as well as other polar vapor analytes such as 1-propanol and piperidine. It is precisely this property of selectively perturbing the intervening dielectric medium (and subsequent conductivity) by incorporating charge-transfer intercalants specific to selected vapor analytes that we exploit to produce highly chemically-selective films.

5. EXPERIMENTAL

From an examination of Eq.(1) over a small temperature range, we can arrive at the following observations for the baseline (i.e. no vapor exposure) conductivity (σ) of a nanocluster film:

$$-\ln\sigma \propto \delta \qquad (4)$$

$$\ln\sigma \propto \frac{-1}{T(^oK)} \qquad (5)$$

where δ is the intercluster spacing.

From an examination of the conductivities of a number of Au:RSH(1:1) films (Fig. 4) where RSH = n-alkyl mercaptans ($C_nH_{2n+1}SH$), we see that the conductivity *decreases* in logarithmic fashion with the number of carbon atoms in the alkyl thiol surfactant. This is precisely what is expected for electron tunneling.

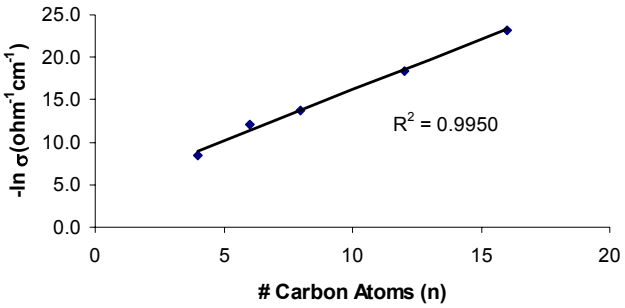

Fig. 4. Conductivities of Au:RSH(1:1) Films @ 25°C.

As further evidenced from the high correlation coefficient (R^2, Fig. 4), the intercluster spacing (Fig. 5) is a near linear function of the number of alkyl carbon atoms.

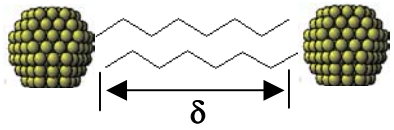

Fig. 5. Intercluster Spacing Parameter.

If we further examine the baseline conductivity of an unexposed nanocluster film as a function of temperature, we observe the following (Fig. 6) relationship:

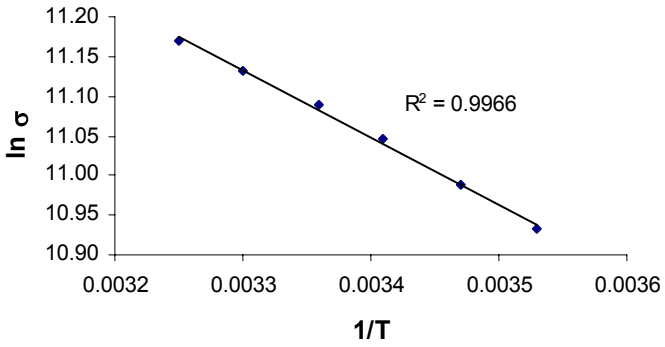

Fig. 6. Arrhenius Plot of Conductivity vs. Temperature of Au:C_2C_6 Film.

As predicted from Eq.(5), the baseline conductivity *increases* in logarithmic fashion with temperature (i.e. with decreasing 1/T). This is characteristic of an electron hopping mechanism.

6. MOLECULAR MECHANISMS

For the cases of TNT and DNT, it is proposed that the presence of strong charge acceptor groups in absorbed vapor molecules results in large changes in the dielectric (and thus the capacitance) of the intercluster medium which produces large changes in the conductivity of the films. This is schematically depicted in Fig. 7 for a Au:C_5COOH monolayer protected nanocluster film.

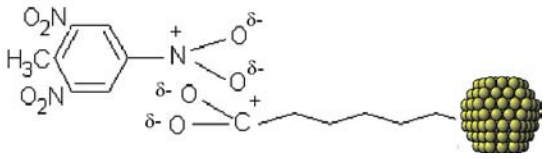

Fig. 7. Interaction of TNT Molecule with Monolayer Protected Nanocluster Film.

To examine this proposition in more detail, we have examined the specific case of DMMP (dimethylmethyl phosphonate, $CH_3(OCH_3)_2P=O$) interaction with a number of different nanocluster films. Fig. 8 depicts the relative resistance changes observed for DMMP and toluene ($CH_3C_6H_5$), normalized to their saturation vapor pressures (P_0) at 25°C.

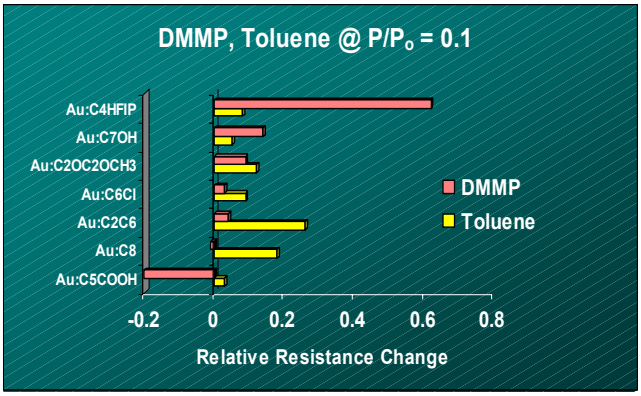

Fig. 8. DMMP and Toluene Vapor Responses to Several Functionalized Nanocluster Films.

One of the results of this examination is the observation that DMMP reacts with a Au:C_5COOH nanocluster film to produce a large *increase* in conductivity (decrease in resistance) from its baseline (no exposure) value. We interpret this increase in conductivity as a consequence of an increase in the intercluster medium dielectric which occurs as a consequence of the formation of hydrogen bonds between the P=O moiety of DMMP and the protons of the COOH acid dimers in the Au:C_5COOH film. Supporting this view are recent infrared reflection-absorption surface studies[26-28] of the interaction of DMMP with $SH(CH_2)_{15}COOH$ monolayers (self-assembled) on planar gold surfaces. Earlier studies[29-30] had pointed to a significant amount of hydrogen-bonding in the form of short linear polymeric chains or "sideways" dimeric structures. Recall that carboxylic acids normally exist as H-bonded dimers in solution and vaporize as such as well. In these surface studies the infrared data indicated that these lateral hydrogen bonds (COOH···COOH) were replaced by hydrogen bonds to DMMP (COOH···O=PX_3). We believe that a similar mechanism occurs in our case (Fig. 9).

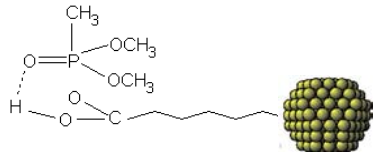

No Vapor → DMMP

(COOH····COOH) → (COOH····O=PX_3)

intra-nanocluster H-bonding

Fig. 9. Interaction of DMMP with Au:C_5COOH Nanocluster Film.

Here the interaction of DMMP with a Au:C_5COOH nanocluster film results in the formation of hydrogen bonds between P=O and the protons of some acid dimers. One result of this is a decrease in intra-nanocluster H-bonding accompanied by a relative *increase* in inter-cluster H-bonding by making the remaining COOH moiety available for such interaction. This would seem to have the overall effect of increasing the dielectric of the intercluster medium and hence increasing the film conductivity (or decreasing the relative film resistance).

In converse fashion the interaction of DMMP with a Au:HFIP film (HFIP = Hexafluoroisopropanol) produces the inverse effect (Fig. 10).

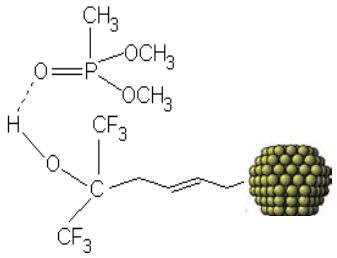

No Vapor → DMMP

$(CF_3COHCF_3 \cdots CF_3COHCF_3)$ → $(CF_3COHCF_3 \cdots O{=}PX_3)$

inter-nanocluster H-bonding

Fig. 10. Interaction of DMMP with Au:HFIP Film.

Here the two bulky –CF_3 groups sterically hinder the formation of any significant amount of intracluster, dimer-like, hydrogen bonding and any H-bonding that occurs would appear to be that of the *intercluster* type. As in the previous case DMMP adsorption also results in the formation of hydrogen bonds between P=O and the hydroxyls of HFIP but now intercluster H-bonding is *decreased* which results in a decrease in the dielectric constant of the intercluster medium. This is reflected in a significant decrease in the baseline film conductivity (or conversely an increase in the film resistance) as shown in Fig. 8.

Toluene vapor, being primarily nonpolar in nature, lacks any capability to form hydrogen bonds as well as significantly perturb the dielectric medium between the nanoclusters. As a result, the response patterns (Fig. 8) indicate *unidirectional* increases in resistance as a result of a film swelling mechanism. The different responses of a particular nanocluster film coating to toluene are determined by toluene vapor's partition coefficient between the gas and coating phases.[31-32]

Currently several charge transfer and hydrogen-bonding reactions between functionalized surfactants and vapors are being explored as one approach to achieving improvements in both sensor selectivity and sensitivity.

7. DEVICE PROTOTYPES

Single chemiresistors consist of interdigitated electrode arrays (2mm X 7mm) with two hundred gold lines with intervening spaces, each 15-microns wide, alternately connected by electrical bus bars. These arrays are fabricated using conventional lithography on quartz substrates, and each transducer occupies a chip area of 14-mm^2 . Multiple arrays are also possible (Fig. 11).

Fig. 11. Close Up Photo of Single and Multiple Microelectrode Arrays Mounted on TO-Headers.

A laboratory prototype handheld detector has recently been fabricated for demonstration purposes (Fig. 12). Using a small, commercial 3V lithium battery, this device will operate *continuously* for a period of 120 hours. With a larger battery, lower-duty cycle on-off times, and optimized power-conditioning its sensing capability can be extended for *years*.

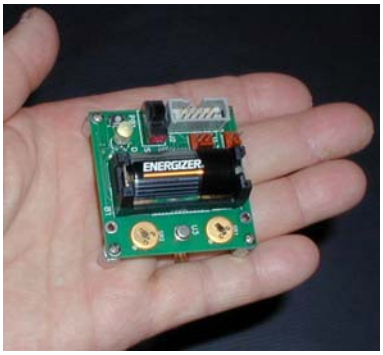

Fig. 12. Handheld Detector (Dual Sensors, Battery, Electronics, LED alarm).

8. CONCLUSION

We have described here a breakthrough technology based on nanoelectronic principles to develop miniature, extremely low-power, chemical sensor systems that respond to environmental vapor signatures of hazardous compounds and TNT/DNT-containing explosives. Their small size, low power (sub-microwatt), rapid response, low-cost (lithographically producible), and humidity-independence are the enabling parameters for an advanced generation of handheld, miniature toxic vapor and explosives detectors with significant improvements in overall system size, weight, power and cost over currently available systems.

ACKNOWLEDGEMENT

This work has been jointly sponsored by the DoD Chemical and Biological Defense Program of the Joint Science and Technology Office and the In-House Laboratory Independent Research (ILIR) program of the Edgewood Chemical Biological Center.

REFERENCES

1. *Nanoscale Materials*, Liz-Marzan, L.M., Kamat P.V., Eds., Kluwer Academic Publishers, Dordrecht, The Netherlands, **2003**.
2. Brust, M.; Walker, M.; Bethell, D.; Schiffrin, D.J.; Whyman, R. *J. Chem. Soc. Chem. Comm*. **1994**, 802.
3. Faraday, M. *Phil. Trans. R. Soc. London* **147**, 145 (1857).
4. Dubois, L.H.; Nuzzo, R.G. *Ann. Revs. Phys. Chem*. **1992**, *63*, 437.
5. Leff, D.V.; Ohara, P.C.; Heath, J.R.; Gelbart, W.M. *J. Phys. Chem.* **1995**, *99*, 7036.
6. Jimenez, V.L.; Leopold, M.C.; Mazzitelli, C.; Jorgenson, J.W.; Murray, R.W.; *Anal. Chem*. **2003**, *75*, 199.
7. Wohltjen, H.; Snow, A.W. *Anal. Chem*. **1998**, *70*, 2856.
8. Snow, A.W.; Wohltjen, H.; Jarvis, N.L.; NRL Review **2002**, 45.
9. Smardzewski, R.R.; Jarvis, N.L.; Snow, A.W.; Wohltjen, H. "Metal-Insulator-Metal Ensemble (MIME) Chemical Detectors", *Nanotech2004 Nanotechnology Conference & Trade Show*, Proceedings Vol. 3, pp. 163- 4, Boston, 7-11 March **2004**.
10. Jarvis, N.L.; Snow, A.W.; Wohltjen, H.; Smardzewski, R.R. "CB Nanosensors", Paper LP-07, 23rd Army Science Conference, 2-5 Dec 2002, Orlando, FL.
11. Snow, H.W.; Wohltjen, H.; *Chem. Mater*. **1998**, *10*, 947.
12. Hostetler, M.J.; Wingate, J.E.; Zhong, C.J.; Harris, J.E.; Vachet, R.W.; Clark, M.R.; Londono, J.D.; Green, S.J.; Stokes, J.J.; Wignall, G.D.; Glish, G.L.; Porter, M.D.; Evans, N.D.; Murray, R.W.; *Langmuir* **1998**, *14*, 17.
13. Hostetler, M.J.; Green, S.J.; Stokes, J.J.; Murray, R.W.; *J. Am. Chem. Soc*. **1996**, *118*, 4212.
14. Hostetler, M.J.; Templeton, A.C.; Murray, R.W.; *Langmuir* **1999**, *15*, 3782.
15. Mitre Technical Report MTR 00B0000014, Sensitivities of Selected Chemical Detectors, February **2000**.
16. Yang, J.S.; Swager, T.M.; *J. Am. Chem. Soc.* **1998**, *120*, 11864.
17. Adams, D. M., et. al., "Charge Transfer on the Nanoscale: Current Status", *J. Phys. Chem. B*, **2003**, *107*, 6668
18. Han, L., Daniel, D. R., Maye, M. M., and Zhong, C., *Anal. Chem*., **2001**, *73*, 4411.
19. Heeger, A. J.; *J. Phys. Chem B*, **2001**, *105*, 8475.
20. Neugebauer, C.A.; Webb, M.B.; *J. Appl. Phys*. **1962**. *33*, 74; Evans, S.D.; Johnson, S.R.; Cheng, Y.L.; Shen, T.; *J. Mater. Chem*. **2000**, *10*, 183.
21. Abeles, B.; Sheng, P.; Coutts, M.D.; Arie, Y.; *Adv. Phys*. **1975**, *24*, 407.
22. Sheng, P.; Abeles, B.; Arie, Y.; *Phys. Rev. Lett*. **1973**, *1*, 44.
23. Sheng, P.; Abeles, B.; *Phys. Rev. Lett*. **1972**, *1*, 34.
24. Cohen, M.H.; Douglas, M.; Currin, N.; Jortner, J.; *Phys. Rev. Lett.* **1973**, *15*, 699.
25. Gittleman, J.I.; Goldstein, Y.;Bozowski, S.; *Phys. Rev. B* **1972**, *9*, 3609.
26. Bertilsson, L.; Engquist, I.; Liedberg, B.; *J. Phys. Chem. B* **1997**, *101*, 6021.
27. Bertilsson, L.; Potje-Kamloth, K.; Liess, H.D.; Engquist, I.; Liedberg, B.; *J. Phys. Chem B* **1998**, *102*, 1260.
28. Bertilsson, L.; Potje-Kamloth, K.; Liess, H.D.; Liedberg, B.; *Langmuir* **1999**, *15*, 1128.
29. Nuzzo, R.G.; Dubois, L.H.; Allara, D.L.; *J. Am. Chem. Soc*. **1987**, *109*, 3559.
30. Smith, E.L.; Alves, C.A.; Anderegg, J.W.; Porter, M.D.; Siperko, L.M.; *Langmuir* **1992**, *8*, 2707.
31. Snow. A.W.; Wohltjen, H.; Anal. Chem. **1984**, *56*, 1411.
32. Grate, J.W.; Nelson, D.A.; Skaggs, R.; Anal. Chem. **2003**, *75*, 1868.